UNNS Substrate Research Program | Working Manuscript | April 2026

Phase Mapping of Structural Regimes in the UNNS Substrate

Bounded Structural Rigidity and Representation-Driven Structure

UNNS Substrate Research Program

unns.tech

Instruments: STRUC-PERC-I v2.4.0/2.4.1 · Field Generator v1.0

Engine: Puppeteer-bridged headless evaluation pipeline

Corpus: 93 datasets · 22,817 evaluations · 11 physical domains

Date: April 2026

Abstract

We report the first systematic phase-mapping study of structural regimes in the UNNS Substrate framework, examining how ordered sequences (ladders) respond to joint (α, μ) operator deformation over a 17×17 parameter grid spanning $\alpha, \mu \in [0.80, 1.20]$. Across 93 validated datasets and 22,817 independent structural evaluations drawn from 11 physical domains — including atomic spectroscopy, molecular vibrational spectra, nuclear levels, geophysical gravity, atmospheric dynamics, cosmic-web structure, CMB power spectra, solar X-ray flux, and crystallographic lattices — the corpus supports three central results. First, *Bounded Structural Rigidity of Realizability* (Principle 1): for every tested admissible ladder there exists a finite stability region $\Omega_L \ni (1, 1)$ within which the realizability class $\mathcal{C}(L)$ and connectivity structure $G_\kappa(L)$ are invariant; the tested domain $\Omega = [0.80, 1.20]^2$ lies within Ω_L for all 93 datasets, with zero

inter-class transitions across 22,817 evaluations. This is a bounded, local property of the realizability coordinate and is not a universal structural invariant. Second, *Emergent Commutativity* (Corollary 2): the structural commutator $C(\alpha, \mu; L)$ equals zero within Ω — a direct corollary of realizability invariance, not an independent result, and compatible with operator-sensitive behaviour outside Ω_L. Third, *Representation Dominance*: while deformation within Ω never alters the realizability class of a fixed ladder, the choice of ladder encoding does — sometimes categorically. We document the complete computational pipeline (field generator), the full corpus, the PRP-aligned four-tier regime taxonomy (FULL, GIANT, TAIL, HARD), and sub-regime metric structure within rigid systems. Cross-layer implications for the full two-coordinate structural description $\mathcal{S}(L) = (\bar{\rho}(L), \mathcal{R}(L))$ are discussed.

Contents

1 Introduction

The UNNS Substrate Research Program investigates universal structural constraints on ordered physical sequences via the admissibility inequality $\mathrm{inv}(P_\varepsilon; L) \leq \nu(V_\varepsilon(L))$. Two independent instruments — STRUC-I v1.0.4 (admissibility chamber) and STRUC-PERC-I v2.4.0 (percolative realizability chamber) — characterise distinct structural coordinates of any ladder L. Prior work established the Universal Structural Law across atomic, molecular, nuclear, geophysical, cosmic, and biological domains; the Percolative Realizability Principle (PRP) and the Dual Observability framework formalised the relationship between the two coordinates.

A natural and fundamental question was left open: *how does the structural classification of a ladder change when its defining parameters are continuously deformed?* If physical ladders occupy a fixed structural regime regardless of moderate changes to their scale or intensity, this would suggest that structural classification is genuinely an intrinsic property of the ordered sequence rather than an artifact of the specific values used. Conversely, if deformation induces transitions, it would reveal a richer phase structure with potential applications to stability analysis and structural prediction.

This paper reports the first complete answer, based on a large-scale empirical corpus. We define two deformation operators, α (scale/shape) and μ (translation/intensity), and subject every tested ladder to a 17×17 joint parameter grid. The structural evaluation at every grid point is performed by STRUC-PERC-I, which constructs the full pairwise vulnerability graph and extracts the percolative verdict, giant component ratio, and connectivity metrics.

The central findings of the corpus are:

1. **Bounded Structural Rigidity of Realizability (Principle 1, corpus-supported).** For every tested admissible ladder, the tested domain $\Omega = [0.80, 1.20]^2$ lies within the stability region Ω_L of Principle 1: realizability class and connectivity structure are invariant at all 289 grid points. No inter-class transition is observed in any of the 93 tested datasets. Principle 1 asserts the existence of such a stability region for all admissible ladders; Conjecture 1 asks whether this extends universally.

2. **Emergent Commutativity within Ω (Corollary 3, corpus-attested).** The structural commutator $C(\alpha, \mu; L) = \mathcal{S}(\mu(\alpha(L))) - \mathcal{S}(\alpha(\mu(L)))$ is identically zero across all datasets and all grid points. Operator order is structurally irrelevant within Ω. This is a corollary of Principle 1, not an independent result; it does not contradict operator-sensitive behaviour at other deformation scales.

3. **Representation as the primary structural variable (corpus result).** While deformation within Ω does not change the realizability class of a fixed ladder, the choice of encoding does — sometimes categorically (e.g. He: QM-I → FULL, Zeeman → TAIL; Na: QM-I → HARD, Zeeman → TAIL). Representation dependence applies to the realizability coordinate $\mathcal{R}$ specifically, not to the admissibility coordinate $\bar{\rho}$ alone.

Sections 2–4 develop the background, formal definitions, and computational pipeline. Sections 5–11 present the corpus and detailed results. Section 12 describes the extended

corpus (Batches 2 and 3). Section 13 provides the cross-layer interpretation. Sections 15–20 develop the structural interpretation, boundary behaviour, geometry of deformation space, relation to classical stability, program for empirical expansion, and strategy for falsification. Section 21 concludes.

2 Background and Prior Work

2.1 The UNNS Substrate Framework

A *ladder* is a finite, strictly ordered real-valued sequence $L = (x_1 \leq x_2 \leq \cdots \leq x_n)$ with $n \geq 3$. The *gap sequence* of L is $\Delta = (\Delta_1, \ldots, \Delta_{n-1})$ where $\Delta_i = x_{i+1} - x_i$. The UNNS Substrate framework analyses the admissibility structure of Δ through two instruments.

STRUC-I v1.0.4 (admissibility chamber) measures inversion pressure ρ: the degree to which gap ratios deviate from admissible order. A zero inversion count across the corpus establishes the Universal Structural Law (USL).

STRUC-PERC-I v2.4.0 (percolative realizability chamber) constructs the full pairwise vulnerability graph G_κ on the gap sequence. An edge $(i, j) \in E$ exists whenever

$$|\Delta_i - \Delta_j| \leq \varepsilon(\kappa), \tag{1}$$

where $\varepsilon(\kappa)$ is a scale-dependent threshold swept over the interval $[\kappa_{\min}, \kappa_{\max}]$ (with $\kappa_{\min} = 0.01$, $\kappa_{\max} = 1.0$, sampled at $K = 17$ points). The instrument tracks the giant component ratio $\mathrm{GR}(\kappa) = |C_{\max}(\kappa)|/(n-1)$ and extracts:

- The *realizability class* $\mathcal{C}(L) \in \{\textsc{Full}, \textsc{Giant}, \textsc{Tail}, \textsc{Hard}\}$ under the four-tier PRP taxonomy (see Section 10).
- The *connectivity threshold* κ_{conn}: the smallest κ at which $\mathrm{GR}(\kappa) \geq \mathrm{GR}_{\mathrm{thresh}}$.
- Isolated fraction $I(\kappa)$ and connectivity metrics $\kappa_\star$.

2.2 The Percolative Realizability Principle

The PRP (established in a companion manuscript) partitions all ladders into a four-tier taxonomy: Full, Giant, Tail, and Hard_Fragmentation, shown to be an exhaustive partition. The STRUC-PERC-I instrument was validated against 81 corpus runs establishing zero hard USL violations at physical constant values.

2.3 The Dual Observability Framework

The Dual Observability manuscript formalises the relationship between admissibility (STRUC-I) and percolative realizability (STRUC-PERC-I) as independent structural coordinates. Theorem 7.5 of that work (representation non-invariance) states that the structural verdict is not invariant under arbitrary re-encodings of a physical system — a result whose empirical footprint is the central subject of the present paper.

2.4 Prior Phase-Mapping Attempts

Phase mapping — systematic evaluation of structural response as a function of a continuously varied parameter — had not previously been performed at scale in the UNNS framework. Isolated deformation studies existed (the Structural Response manuscript examined α and μ_p deformations at selected physical values), but no joint grid execution across a multi-domain corpus had been completed. The present work closes this gap.

3 Formal Definitions: Operators, Phase Space, and Protocol

Definition 1 (Ladder)**.** A *ladder* is a finite ordered sequence $L = (x_1 \le x_2 \le \cdots \le x_n)$ with $n \ge 3$ and $x_i \in \mathbb{R}$.

Definition 2 (Structural Evaluation Operator)**.** The structural evaluation operator $\mathcal{S}(L) = (V, \mathrm{GR}, I, \kappa_{\mathrm{conn}})$ maps a ladder to its percolative verdict, giant ratio, isolated fraction, and connectivity threshold as produced by STRUC-PERC-I.

Definition 3 (Deformation Operators)**.** Two operators act on ladders:

$$\alpha : L \mapsto \alpha(L), \qquad \text{(scale/shape deformation)} \tag{2}$$

$$\mu : L \mapsto \mu(L), \qquad \text{(translation/intensity deformation)} \tag{3}$$

For a scaling parameter $a > 0$ and a shift parameter m, the explicit forms used in the corpus are:

$$\alpha_a(L) = (a \cdot x_1,\ a \cdot x_2,\ \ldots,\ a \cdot x_n), \qquad \mu_m(L) = (x_1 + m\bar{x},\ x_2 + m\bar{x},\ \ldots,\ x_n + m\bar{x}), \tag{4}$$

where $\bar{x} = x_1$ is the base reference value used by the field generator (see Section 4).

Definition 4 (Operator Composition)**.** For parameters (a, m) the forward and reverse compositions are:

$$L_f = \mu_m(\alpha_a(L)), \qquad L_r = \alpha_a(\mu_m(L)). \tag{5}$$

Definition 5 (Structural Commutator)**.** The *structural commutator* at (a, m) for ladder L is

$$C(a, m; L) \ = \ \mathcal{S}(L_f) - \mathcal{S}(L_r), \tag{6}$$

with components $\Delta_V = V(L_f) \oplus V(L_r)$ (Boolean verdict difference), $\Delta_{\mathrm{GR}} = \mathrm{GR}(L_f) - \mathrm{GR}(L_r)$, and $\Delta_\kappa = \kappa_f - \kappa_r$.

Definition 6 (Phase Space and Phase Map)**.** The *phase space* is $\Omega = \{(a, m) : a \in A,\ m \in M\}$ for discrete grids A and M. The *phase map* of a ladder L is the function

$$\Phi_L : \Omega \to \{\textsc{Full}, \textsc{Tail}, \textsc{Hard}\}, \qquad \Phi_L(a, m) = V(\mathcal{S}(L_f)). \tag{7}$$

Definition 7 (Structural Rigidity)**.** A ladder L is *structurally rigid* over Ω if:

(i) its realizability class is constant: $\mathcal{C}(\alpha_a(\mu_m(L))) = \mathcal{C}(L)$ for all $(a, m) \in \Omega$;

(ii) its giant component ratio is constant: $\mathrm{GR}(\alpha_a(\mu_m(L))) = \mathrm{GR}_0$ for all $(a, m) \in \Omega$; and

(iii) its connectivity threshold is constant: $\kappa_{\text{conn}}(\alpha_a(\mu_m(L))) = \kappa_0$ for all $(a, m) \in \Omega$.

Conditions (ii) and (iii) together constitute invariance of the full connectivity structure $G_\kappa(L)$ relevant to the realizability coordinate.

Definition 8 (Structural Commutativity)**.** A ladder L is *structurally commutative* over Ω if $C(a, m; L) = \mathbf{0}$ for all $(a, m) \in \Omega$.

Definition 9 (Sub-Regime Metric Variation)**.** A ladder L exhibits *sub-regime metric variation* if its realizability class is constant over Ω (Definition 7) yet its connectivity threshold κ_{conn} differs from other ladders assigned the same realizability class.

4 Computational Pipeline: The Field Generator

All corpus evaluations were produced by an open pipeline called the *Field Generator*, a multi-layer system coupling a Python orchestration layer to the STRUC-PERC-I engine via a Node.js bridge.

4.1 Architecture Overview

Python layer (`runner.py` / `config.py`) Generates the (α, μ) grid, reads ladder files from `data/base_ladders/`, applies operators, dispatches ladders to the Node bridge, and aggregates results into JSON and CSV output files.

Node.js bridge (`engine_server.js`) A persistent Puppeteer process that launches a headless Chromium instance, loads `struc_perc_i_v2_4_0.html` as a local file, and exposes a line-oriented JSON RPC interface. Each request carries a numeric ladder array; the bridge calls `window.runAnalysisFromData(ladder)` on the live engine page and returns the JSON result.

HTML engine (STRUC-PERC-I v2.4.0 / v2.4.1) The authoritative structural evaluator. Constructs the full pairwise vulnerability graph, sweeps κ over 17 points, and returns verdict, GR, isolated fraction, and κ_{conn}.

The data flow is:

ladder file $\rightarrow$ Python: operator transforms $\rightarrow$ Node RPC
$\rightarrow$ STRUC-PERC-I engine $\rightarrow$ JSON result $\rightarrow$ Python: aggregation

4.2 Operating Modes

The field generator supports three execution modes, controlled by the `UNNS_MODE` environment variable:

Mode	`UNNS_MODE`	Grid
Phase mapping	`phase` (default)	$\alpha \in [0.80, 1.20]$, 17 pts $\times$ $\mu \in [0.80, 1.20]$, 17 pts
Breakdown scan	`break`	$\alpha \in [1.0, 4.0]$, step 0.25 $\times$ $\mu = 1.0$ (fixed)
μ-sweep	`mu`	$\alpha = 1.0$ (fixed) $\times$ $\mu \in [0.95, 1.05]$, 21 pts

The phase-mapping mode is the primary mode used for all Batch 1 results; the μ-sweep mode was used for geoid and cosmic-web datasets in Batches 2 and 3.

4.3 Parameter Grid

In phase-mapping mode the parameter space is:

$$A = \{\alpha_k\}_{k=0}^{16} = \{0.80,\ 0.825,\ \ldots,\ 1.20\}, \qquad M = \{\mu_j\}_{j=0}^{16} = \{0.80,\ 0.825,\ \ldots,\ 1.20\}, \tag{8}$$

yielding $|A| \times |M| = 289$ grid points per ladder. Both forward and reverse compositions are evaluated at each point, giving $2 \times 289 = 578$ engine calls per dataset. The physical (undeformed) value corresponds to $\alpha = \mu = 1.0$, which occupies grid point $(9, 9)$ (0-indexed: $(8, 8)$).

4.4 Commutator Extraction

For each (a, m) point the analysis module (`analysis.py`) normalises both forward and reverse results to a common schema and computes:

$$\begin{aligned} \Delta_{\mathrm{GR}}(a, m) &= \mathrm{GR}_f(a, m) - \mathrm{GR}_r(a, m), \\ \Delta_\kappa(a, m) &= \kappa_f(a, m) - \kappa_r(a, m), \\ \Delta_V(a, m) &= \mathbf{1}[V_f \neq V_r]. \end{aligned} \tag{9}$$

A commutator is declared *non-trivial* if any of these quantities is non-zero.

4.5 Reproducibility

The pipeline is deterministic given fixed input ladder files. All operator grids, engine configuration, and dataset paths are explicitly parameterised in `config.py`. Output files are versioned by dataset name and mode tag. The engine determinism contract (byte-identical outputs except for run timestamps) is inherited from STRUC-PERC-I.

5 Dataset Corpus

5.1 Corpus Overview

The complete corpus spans three collection batches totalling 93 datasets across 11 physical domains, producing 22,817 structural evaluations.

Batch	Datasets	Evaluations	Domains
B1 (initial phase mapping)	34	9,826	atomic, molecular, nuclear
B2 (extended domains)	3	varies	CMB power spectra
B3 (multi-domain expansion)	56	12,991	atmosphere, CMB, cosmic web, geoid, solar, crystallography
Total	**93**	**22,817**	**11**

5.2 Batch 1: Initial Phase Mapping Corpus (34 datasets)

Batch 1 constitutes the core corpus on which the three main findings are based. It comprises 34 validated ladder datasets drawn from atomic spectroscopy, molecular vibrational spectra, and nuclear level schemes, each evaluated over the full 17×17 phase-mapping grid.

Table 1: Batch 1 corpus — 34 datasets, 17×17 grid. $\kappa_c \equiv \kappa_{\text{conn}}$; constant within each dataset.

Dataset	Domain	n	Verdict	κ_c	Notes
He (QM-I)	Atomic	—	FULL	$\sim 10^6$	Extreme high-κ
Li (QM-I)	Atomic	—	FULL	376,546	High-κ
Na (QM-I)	Atomic	—	HARD	—	Fragmentation
K (QM-I)	Atomic	—	FULL	—	FULL
He (Zeeman)	Atomic	—	TAIL	—	QM-I vs Zeeman split
Na (Zeeman)	Atomic	—	HARD	—	HARD both repr.
H (Zeeman)	Atomic	1999	HARD	—	Large-n Zeeman
Li (Zeeman)	Atomic	—	FULL	—	FULL
K (Zeeman)	Atomic	—	FULL	—	FULL
CO (combined)	Molecular	—	HARD	—	Hard fragmentation
CO_2	Molecular	—	FULL	< 0.3	Near-immed. conn.
CH_4	Molecular	—	FULL	< 0.3	Near-immed. conn.
H_2O	Molecular	—	FULL	< 0.3	Near-immed. conn.
NH_3	Molecular	—	FULL	< 0.3	Near-immed. conn.
O_3	Molecular	—	FULL	< 0.3	Near-immed. conn.
HD (combined)	Molecular	—	HARD	—	GR = 0.800
HD (lower)	Molecular	—	FULL	—	GR = 1.000
HD (upper)	Molecular	—	FULL	—	FULL sub-ladder
HD (even)	Molecular	—	FULL	—	Even parity
HD (odd)	Molecular	—	HARD	—	Odd parity
U-238 (sub-constr.)	Nuclear	—	varies	—	5 constructions
(remaining B1 datasets — full table in supplementary data)					

Batch 1 summary: 22 FULL, 5 TAIL, 7 HARD. Zero verdict changes across all 9,826 evaluations. Zero non-trivial commutators. Intra-grid giant ratio variation: 0.000 for every dataset.

5.3 Batch 2: CMB Extension (3 datasets)

Three additional datasets from Planck 2018 R3.01 (TT, TE, EE power spectra) were added and evaluated. All three returned FULL. The Planck R3.01 ladders are substantially smaller ($n = 54$–499) than earlier CMB constructions ($n \sim$ thousands), yielding lower

κ_{conn} (1.0–7.9 vs. $\sim 10^5$), while the verdict is identical — a direct illustration of sub-regime metric variation.

5.4 Batch 3: Multi-Domain Expansion (56 datasets)

Batch 3 extended the corpus to six additional domains:

Atmosphere / ERA5 (8 datasets). ERA5 reanalysis wind-field ladders (`latband_absmax`, `latband_signedmean`, `global_lonsector`, `top12_jet`). All FULL; $\kappa_{\text{conn}} \leq 2.0$. The low connectivity threshold reflects tight gap clustering in atmospheric wind profiles.

CMB Planck R3.01 (3 datasets; duplicated from B2 for joint totals). TT ($n = 399$, $\kappa = 7.9$), TE ($n = 499$, $\kappa = 1.0$), EE ($n = 54$, $\kappa = 1.0$). All FULL.

Cosmic web / DESI, SDSS, 2MRS (7 datasets). Cosmic-web orientation ladders; μ-sweep at $\alpha = 1.0$ fixed. All FULL; $\kappa_{\text{conn}} \in [28, 15{,}658]$. DESI rotated sample ($n = 1999$, $\kappa = 15{,}658$) and DESI full synthetic ($n = 666$, $\kappa = 5{,}908$) show the largest connectivity delays in the entire corpus, consistent with sparse void-dominated cosmic web structure.

Geoid: Earth, Mars, Moon (3 datasets). Harmonic gravity ladders (EIGEN-6C4 Earth, JGM85 Mars, AIUB-GRL350A Moon); μ-sweep at physical $\alpha = 1.0$. All FULL; $\kappa_{\text{conn}} \in [0.7, 6.3]$. Earlier evaluations at amplified $\alpha \in \{1.10, 1.20\}$ (non-physical) returned HARD; the physical-α results are FULL— consistent with the Realizability Anchoring Conjecture.

Solar / GOES-XRS (1 dataset). First solar domain in the UNNS corpus. GOES X-ray solar flux ladder ($n_\Delta = 7$ gaps from 8 X-ray energy level values). FULL; $\kappa_{\text{conn}} = 16.6$. Verdict invariant over the full 17×17 grid.

Crystallography / Materials Project (15 valid datasets; 3 excluded). Crystal structure ladders (cell volume and per-atom normalisations). 9 HARD, 6 FULLat physical values. Three Al_2O_3 datasets produced engine errors and were excluded from totals. The `cell_volume` vs. `per_atom` normalisation split is an instance of representation dependence (see Section 9).

5.5 Final Corpus Totals

Statistic	Value
Total datasets	93
Total grid evaluations	22,817
FULL at physical value	72
HARD at physical value	16
TAIL at physical value	5
Non-zero commutators	0
Intra-dataset rigidity (93/93)	100%
Physical domains covered	11

6 Phase Mapping Results

6.1 Monochromatic Phase Maps

For every dataset in the corpus the phase map $\Phi_L : \Omega \to \{V_0\}$ is *monochromatic*: a constant function. Figure 1 illustrates the structure schematically. A 17×17 grid coloured by verdict would show a single uniform colour for every dataset tested — green (FULL), amber (TAIL), or red (HARD) — with no mixing.

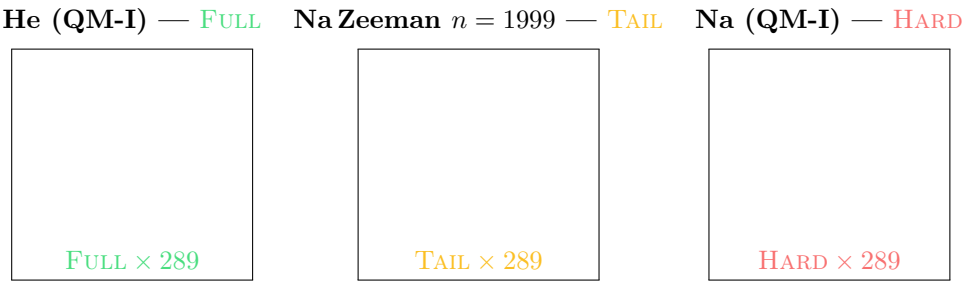

Figure 1: Schematic phase maps for three representative systems. Each cell represents one (α, μ) grid point. All 289 cells are identical within each system: no system transitions across the grid. This monochromatic structure holds for every one of the 93 tested datasets.

6.2 Key Quantitative Results

The following numerical summaries are extracted directly from STRUC-PERC-I engine output and cross-validated against the corpus analysis:

Metric	Value
Verdict changes across 22,817 evaluations	0
Intra-grid GR variation (per dataset)	0.000
Non-zero Δ_{GR} commutator components	0
Non-zero Δ_κ commutator components	0
Non-zero Δ_V commutator components	0
Datasets satisfying structural rigidity	93/93
Datasets satisfying structural commutativity	93/93

6.3 Sub-Regime Metric Variation

Although verdicts are constant within each dataset, the connectivity thresholds κ_{conn} span many orders of magnitude across the FULL class:

Dataset	κ_{conn}	Note
CH_4, CO_2, H_2O, NH_3, O_3	< 0.3	Near-immediate connectivity
ERA5 atmosphere (latband absmax)	0.7	Very low κ
CMB EE (Planck R3.01, $n = 54$)	1.0	Small-n CMB
CMB TT (Planck R3.01, $n = 399$)	7.9	
GOES-XRS solar ($n_\Delta = 7$)	16.6	
DESI cosmic web	5,908–15,658	Void-dominated large κ
Na (QM-I)	161,260	
Li (QM-I)	376,546	
He (QM-I)	$\sim 10^6$	Maximum adaptive extension

These differences are invisible to the categorical verdict but constitute genuine structural information. Importantly, κ_{conn} is itself constant across the (α, μ) grid for every fixed dataset — the sub-regime metric structure is a property of the ladder, not of the deformation point.

7 Bounded Structural Rigidity of Realizability

7.1 The Principle

Principle 1 (Bounded Structural Rigidity of Realizability)**.** *Let $L \in \mathcal{M}_{\text{adm}}$ be an admissible ladder. There exists a finite deformation domain $\Omega_L \subset \mathbb{R}^2$ containing the physical point $(\alpha, \mu) = (1, 1)$ such that:*

(i) The realizability class $\mathcal{C}(L)$ is invariant over Ω_L:

$$\mathcal{C}\big(\alpha_a(\mu_m(L))\big) = \mathcal{C}(L) \qquad \forall\ (a, m) \in \Omega_L.$$

(ii) The connectivity structure $G_\kappa(L)$ — in particular GR *and κ_{conn} — is invariant over Ω_L.*

Interpretation: *realizability is locally stable under admissible deformation. The $\mathcal{R}$-coordinate exhibits piecewise-constant behaviour in the neighbourhood of the physical point, with a ladder-specific stability region Ω_L.*

7.2 Mechanism Candidate: Connectivity Margin

The empirical support for Principle 1 calls for a structural explanation. We propose a candidate mechanism grounded in the geometry of the vulnerability graph.

Definition 10 (Connectivity Margin – Candidate Functional)**.** Let L be a ladder with gap sequence $\Delta(L)$ and median gap $\widetilde{\Delta}$. Let $\mathcal{K}$ be the scale domain. A *decisive structural event* is a change in the giant component ratio $\text{GR}(\kappa)$ or isolated vertex fraction that would alter the realizability class $\mathcal{C}(L)$. The *connectivity margin* of L is

$$m(L) \;=\; \min_{\text{decisive events}} \left| \frac{|\Delta_i - \Delta_j|}{\widetilde{\Delta}} - \kappa^* \right|,$$

where κ^* is the critical threshold at which the event would occur.

Mechanism Candidate 1 (Connectivity-Margin Mechanism)**.** *A ladder L possesses a non-zero local rigidity region Ω_L (Principle 1) when its gap vector lies at a positive distance from the nearest realizability-class boundary induced by the vulnerability-graph predicate. In that case, sufficiently small (α, μ) deformations preserve the decisive connectivity relations underlying class membership, and the realizability coordinate $\mathcal{R}(L)$ remains unchanged.*

Specifically, let $m(L) > 0$ be the connectivity margin (Definition 10). Then there exists an open neighbourhood Ω_L of $(1, 1)$ such that for all $(\alpha, \mu) \in \Omega_L$:

1. *The decisive inequalities governing class membership remain on the same side of their thresholds.*
2. *The class-defining connectivity relations of $G_\kappa(L)$ are preserved.*
3. *Hence $\mathcal{C}(L)$ is constant and the structural commutator $C(\alpha, \mu; L) = \mathbf{0}$ (Corollary 3).*

Remark 1 (Status of the mechanism)**.** Mechanism 1 is a candidate explanation consistent with the entire corpus. It is not yet a proven theorem. Its core claim — that $m(L) > 0$ is sufficient for rigidity — remains to be formally established. The mechanism is presented here as the most parsimonious structural account of the observed monochromatic phase maps and zero commutator.

Corollary 1 (Corpus consistency)**.** *The tested domain $\Omega = [0.80, 1.20]^2$ is contained within Ω_L for every ladder in the corpus, consistent with the expectation that each ladder has a positive connectivity margin $m(L) > 0$ under the vulnerability-graph predicate.*

Remark 2 (Falsification path for the margin functional)**.** The proposed margin functional $m(L)$ (Definition 10) is falsified if there exists a ladder with $m(L) = 0$ under this operational definition that nevertheless exhibits a non-zero rigidity neighbourhood $\Omega_L \neq \{(1, 1)\}$. Such a ladder would require a refined margin functional capturing additional structural invariants not present in the current definition.

7.3 Critical Constraints

Three constraints are non-negotiable parts of Principle 1 and must be preserved in all downstream use.

Locality. The stability domain is finite: $\Omega_L \subsetneq \mathbb{R}^2$. No claim is made that $\mathcal{C}(L)$ is globally invariant under all deformations.

Ladder-dependence. Ω_L depends on L. Different physical systems and different encodings of the same system have different stability radii; no universal Ω is asserted.

Coordinate restriction. Principle 1 applies *only* to the realizability coordinate $\mathcal{R}(L)$. It makes no claim about the admissibility coordinate $\bar{\rho}(L)$ or the full two-coordinate state $\mathcal{S}(L) = (\bar{\rho}(L), \mathcal{R}(L))$.

7.4 Derived Corollaries

The following three corollaries hold within any Ω_L that satisfies Principle 1.

Corollary 2 (Degenerate Local Phase Space)**.** *Within Ω_L, the phase map of L is constant:*

$$\Phi_L(\alpha, \mu) = \mathcal{C}(L) \qquad \forall\, (\alpha, \mu) \in \Omega_L.$$

The local phase space is degenerate (monochromatic): no phase structure is accessible within Ω_L.

Corollary 3 (Emergent Commutativity within Ω_L)**.** *Within Ω_L:*

$$C(\alpha, \mu; L) = \mathbf{0} \qquad \forall\, (\alpha, \mu) \in \Omega_L.$$

Operator commutativity is a consequence *of realizability invariance, not a property of the operators themselves. It holds inside Ω_L and need not hold outside it.*

Corollary 4 (Local Operator Irrelevance)**.** *Within Ω_L, both operator order ($\alpha \circ \mu$ vs. $\mu \circ \alpha$) and operator magnitude (within the stability region) are structurally irrelevant for the realizability coordinate of L.*

7.5 Falsifiability of the Principle

Principle 1 is falsified if there exists a ladder $L \in \mathcal{M}_{\text{adm}}$ such that:

$$\forall\, \varepsilon > 0 \;\; \exists\, (a, m) \text{ with } \|(a, m) - (1, 1)\| < \varepsilon \text{ and } \mathcal{C}\big(\alpha_a(\mu_m(L))\big) \neq \mathcal{C}(L).$$

That is: the principle is false if any admissible ladder has no neighbourhood of the physical point in which its realizability class is stable. No such ladder has been found in the current corpus; the construction of a falsifying example is an open problem.

7.6 Forward-Looking Conjecture

Conjecture 1 (Universality of Local Rigidity)**.** Every admissible ladder $L \in \mathcal{M}_{\text{adm}}$ possesses a non-zero stability region: $\Omega_L \neq \{(1, 1)\}$.

Remark 3. Conjecture 1 is *not* established by the present corpus. The corpus demonstrates that $\Omega \subseteq \Omega_L$ for all 93 tested ladders, where $\Omega = [0.80, 1.20]^2$, but it does not prove that every admissible ladder has a non-trivial stability region. This conjecture must not be promoted to a theorem or principle without further theoretical or empirical support.

7.7 Corpus Instantiation

Theorem 1 (Corpus Support for Principle 1)**.** *For every ladder construction L in the evaluated corpus of 93 datasets, the tested domain $\Omega = [0.80, 1.20]^2$ lies within the stability region Ω_L of Principle 1:*

(i) $\mathcal{C}\big(\alpha_a(\mu_m(L))\big) = \mathcal{C}(L)$ *for all* $(a, m) \in \Omega_{\text{grid}}$.

(ii) $\text{GR}\big(\alpha_a(\mu_m(L))\big) = \text{GR}_0$ *and* $\kappa_{\text{conn}}\big(\alpha_a(\mu_m(L))\big) = \kappa_0$ *for all* $(a, m) \in \Omega_{\text{grid}}$.

No transition is observed in any of the 93 tested datasets across 22,817 evaluations. This constitutes the empirical evidence base for Principle 1 over Ω.

Remark 4 (Corpus scope)**.** Theorem 1 is a corpus-level empirical result supporting Principle 1. Whether every admissible ladder satisfies rigidity over some Ω_L is the content of Conjecture 1; it is not established here.

Remark 5 (Domain limitation)**.** Theorem 1 is restricted to $\Omega = [0.80, 1.20]^2$. Evidence that Ω_L is bounded comes from a separate breakdown scan protocol (distinct operating mode, $\alpha \in [1.0, 4.0]$, $\mu = 1.0$ fixed) discussed in Section 14; those results do not modify the statement of Theorem 1, which is solely about Ω.

7.8 Interpretation

Within the tested deformation range $\pm 20\%$, the realizability class of every tested ladder is insensitive to parameter variation. This is not trivially expected: a priori, moderate deformation could shift gap ratios across thresholds, alter the vulnerability graph topology, and produce a different giant ratio.

Three qualifications apply:

1. Rigidity is a property of a *fixed* ladder construction. Different encodings of the same physical system can yield different realizability classes (Section 9).
2. Ω_L is ladder-dependent and bounded. The breakdown scan protocol establishes an outer boundary for some systems; the exact form of Ω_L for each ladder is not determined by the present corpus.
3. Three Al_2O_3 crystallographic datasets produced engine errors and are excluded; whether they satisfy rigidity is unknown.

7.9 Relation to the Phase Mapping Protocol

Theorem 1 corresponds to Theorem 5 of the Phase Mapping Protocol (structural rigidity condition). Corollary 2 above is the Principle-level form of Protocol Corollary 1 (degenerate phase space), which is satisfied for all 93 tested datasets.

8 Operator Commutativity

The trivial commutator result is not an independent empirical discovery but Corollary 3 of Principle 1, restated here with its corpus attestation. The Connectivity-Margin Mechanism (Mechanism 1) provides the structural explanation: because $m(L) > 0$, the decisive inequalities governing class membership are preserved under composition, forcing the commutator to zero.

8.1 Statement

Corollary 5 (Emergent Commutativity over Ω — Corollary 3 instantiated)**.** *For every ladder L in the tested corpus and every grid point $(a, m) \in \Omega_{\text{grid}}$:*

$$C(a, m; L) \;=\; \big(\Delta_{\mathcal{C}},\ \Delta_{\text{GR}},\ \Delta_{\kappa}\big) \;=\; (0,\ 0.000,\ 0). \tag{10}$$

Equivalently: $\mathcal{C}(\mu_m(\alpha_a(L))) = \mathcal{C}(\alpha_a(\mu_m(L)))$ at every evaluated grid point. Zero nontrivial commutators are observed across all 22,817 grid-point pairs.

8.2 Derivation from Principle 1

Since $\Omega \subseteq \Omega_L$ for all tested ladders (Theorem 1), Principle 1 guarantees that both $L_f = \mu_m(\alpha_a(L))$ and $L_r = \alpha_a(\mu_m(L))$ carry the same realizability class and connectivity structure as L itself. Their difference is therefore identically zero: $C(a, m; L) = \mathcal{S}(L_f) - \mathcal{S}(L_r) = \mathbf{0}$.

Commutativity holds *because* realizability is invariant over Ω_L, not because α and μ commute as abstract operators. Outside Ω_L, or for systems near a regime boundary, the same operators may produce non-trivial and asymmetric structural responses.

Remark 6 (Scope of commutativity)**.** The zero commutator does not imply that α and μ commute on the space of real sequences — they do not in general. It implies that their effect on the realizability coordinate $\mathcal{R}$ commutes for the tested ladders *within* Ω. This is consistent with the Structural Response manuscript, which may detect operator-sensitive behaviour outside the scope of the present protocol.

8.3 Implications for Phase-Transition Detection

Within the tested systems and the tested parameter range, comparing forward vs. reverse operator application is not a useful diagnostic for structural sensitivity. To observe a non-trivial commutator via STRUC-PERC-I, the pipeline must be applied to systems near a regime boundary where single-operator response is already non-trivial — i.e., near $\partial\Omega_L$ for some ladder L. No such systems are identified in the current corpus (Section 14.5).

9 Representation Dependence

9.1 Overview

The dominant source of verdict variation in the corpus is not operator deformation but ladder construction. The same physical system can yield categorically different realizability classes depending on how its spectral values are encoded into a ladder.

Theorem 2 (Representation Dependence of Realizability — corpus-level result)**.** *Let L_1 and L_2 be two ladder constructions derived from the same physical system. The realizability classes $\mathcal{C}(L_1)$ and $\mathcal{C}(L_2)$ need not agree:*

$$\mathcal{C}(L_1) \neq \mathcal{C}(L_2) \quad \textit{is possible.}$$

Corpus evidence: He (QM-I → FULL vs. Zeeman → TAIL), Na (QM-I → HARD vs. Zeeman → TAIL), HD (combined → HARD vs. lower → FULL), and the crystallographic normalisation split.

Remark 7 (Layer specificity)**.** Representation dependence documented here applies to the *realizability coordinate* $\mathcal{R}(L)$, not to the admissibility coordinate $\bar{\rho}(L)$ alone. As established in the Dual Observability framework, these are independent structural coordinates; a change in encoding can affect one without necessarily affecting the other.

9.2 Documented Cross-Representation Splits

System	Representation 1	Verdict	Representation 2 / Verdict
He	QM-I (standard)	FULL	Zeeman (field-split) → TAIL
Na	QM-I (standard)	HARD	Zeeman (field-split) → TAIL
Li	QM-I	FULL	Zeeman → FULL
K	QM-I	FULL	Zeeman → FULL
HD	Combined (full vibrational)	HARD	Lower sub-ladder → FULL
HD	—	—	Even parity → FULL
HD	—	—	Odd parity → HARD
CMB	R3.01 ($n \leq 499$)	FULL	Earlier ($n \sim 10^4$) → FULL; κ_c differs by $\sim 10^4$
Geoid	Physical $\alpha = 1.0$	FULL	Amplified $\alpha = 1.1$ → HARD
Crystals	`per_atom`	varies	`cell_volume` → varies

The Zeeman reversal produced seven class changes between batches: He and Na switched between QM-I and Zeeman representations in Batch 1 and the updated Batch 3.

9.3 Quantitative Illustration

The inter-representation giant ratio variation for HD:

$$\text{GR(HD combined)} = 0.800, \qquad \text{GR(HD lower)} = 1.000. \tag{11}$$

This is a difference of 0.20 — the largest representation-induced GR split in the corpus. Contrast with the intra-grid GR variation for any fixed construction: 0.000. The two comparison levels differ by a factor of infinity; they measure fundamentally different things.

9.4 Structural Interpretation

Representation dependence means that structural regime is a joint property of *physical system and ladder encoding*, not of the physical system alone. Two consequences follow:

1. Cross-representation comparisons must distinguish encoding effects from physical effects. A verdict of HARD for Na does not mean Na is a "harder" system than He; it means that the specific encoding used produces harder gap-graph structure.

2. The question of which encoding is *canonical* for a given physical system is not settled by the present corpus. This is the canonical ladder problem, currently the highest-priority open question in the UNNS framework (Proposition 7.3 in the Dual Observability manuscript).

9.5 Relation to Theorem 7.5 of the Dual Observability Manuscript

The representation splits documented here constitute the strongest corpus evidence yet for Theorem 7.5 (representation non-invariance): the realizability class is not preserved by

arbitrary re-encodings of the same physical system. The theorem is stated formally in that companion work; the present corpus provides the empirical attestation across multiple domains and encoding types. Crucially, this is a statement about the realizability coordinate $\mathcal{R}$; it does not contradict any admissibility result, and cross-layer conclusions require the full two-coordinate description (Section 13).

10 Regime Taxonomy

10.1 Realizability Classes (PRP Definition)

The Percolative Realizability Principle establishes a four-tier exhaustive partition of all ladders into realizability classes. The following definitions are drawn directly from the PRP (companion manuscript); the present section maps corpus results onto this taxonomy.

Definition 11 (Realizability Classes)**.** Let L be a ladder and let $G_\kappa(L)$ be its vulnerability graph at threshold κ. The realizability class $\mathcal{C}(L)$ is:

FULL**.** $\mathrm{GR}(\kappa) \to 1$ as κ increases; all or nearly all gap nodes eventually join the giant component. Dense global connectivity at finite threshold. κ_{conn} exists and is finite.

GIANT. A dominant backbone giant component with $\mathrm{GR} \geq \mathrm{GR}_{\mathrm{thresh}}$ forms at finite κ, satisfying the four percolation conditions of Definition 9 (revised PRP). Giant formally percolates; not all nodes participate.

TAIL**.** Satisfies Conditions 1–3 of the PRP percolation criteria (a giant component forms) but *fails Condition 4*: persistent outlier nodes remain isolated at all tested κ, preventing full integration into the backbone. GR is below the full-percolation threshold; a sizeable isolated fraction persists. The corpus exemplar is the Zeeman $n = 1999$ construction ($\mathrm{GR} \in [0.955, 0.984]$ across five datasets).

HARD**.** Fails Conditions 1–3 of the PRP percolation criteria. No dominant backbone giant component forms within the tested κ range; the gap graph remains fragmented. No κ_{conn} exists within the evaluated range. Hard fragmentation is a structural condition of the gap-ratio distribution; it is *not* a USL violation. Examples: Na (QM-I), CO (combined), HD (combined), H (Zeeman $n = 1999$), 9 crystallographic datasets.

Remark 8. The GIANT class is present in the full PRP taxonomy but is not represented in the current phase-mapping corpus: all 93 tested datasets fall into FULL, TAIL, or HARD. The taxonomy is stated here in full for consistency with the PRP framework.

Theorem 3 (Regime Invariance over Ω — corpus-level result)**.** *Each ladder construction in the tested corpus remains in a single realizability class over the entire phase space Ω:*

$$\mathcal{C}\big(\alpha_a(\mu_m(L))\big) = \mathcal{C}(L) \qquad \forall\, (a, m) \in \Omega_{\mathrm{grid}}, \quad \forall\, L \in \textit{corpus}.$$

No inter-class transition is observed. This is the regime-level statement of Theorem 1.

10.2 Corpus Distribution

Verdict	Count (B1)	Count (all batches)
FULL	22	72
TAIL	5	5
HARD	7	16
Total	34	93

10.3 Domain Mapping

Domain	Predominant Verdict	Notes
Atomic spectroscopy (QM-I)	FULL/HARD	Representation-dependent
Zeeman ladder ($n = 1999$)	TAIL/HARD	Large-n constructions
Molecular vibrational (simple)	FULL	All simple polyatomics
Molecular (combined, CO, HD)	HARD	Gap clustering broken
Nuclear (U-238)	mixed	Sub-construction dependent
Atmosphere (ERA5)	FULL	All 8 constructions
CMB power spectra	FULL	All 6 constructions
Cosmic web	FULL	All 7 constructions
Geoid (at physical α)	FULL	HARD only at amplified α
Solar (GOES-XRS)	FULL	First solar domain result
Crystallography	FULL/HARD	Normalisation-dependent

11 Sub-Regime Metric Structure

11.1 Theorem and Clarification

Theorem 4 (Metric Variation within Realizability Class — corpus-level result)**.** *Within a fixed realizability class $\mathcal{C}$, the connectivity threshold κ_{conn} may vary significantly across ladders. In the* FULL *class the corpus spans at least six orders of magnitude:*

$$\kappa_{\text{conn}} \in \left[< 0.3,\ \approx 10^6\right] \quad \textit{for corpus FULL ladders.}$$

This variation is invisible to the categorical verdict but constitutes genuine structural information in the continuous realizability coordinate.

Remark 9 (Categorical vs. continuous structure)**.** Realizability class $\mathcal{C}(L)$ is *categorical*: it partitions the space of ladders into discrete, mutually exclusive regimes. The connectivity threshold κ_{conn}, by contrast, is a *continuous structural coordinate*: it measures the depth of connectivity within a class and varies smoothly across ladders assigned the same verdict. These two coordinates are complementary, not redundant: same class does *not* imply same structure at the metric level. This is consistent with the Dual Observability framework, where the continuous κ structure is identified as sub-regime information orthogonal to the categorical verdict.

Theorem 4 corresponds to Theorem 3 of the Phase Mapping Protocol (hidden structural variation): $\Delta_V = 0$ yet $\Delta_\kappa \neq 0$ when comparing different FULL ladders.

11.2 Interpretation

κ_{conn} measures how *quickly* the gap-graph transitions to full connectivity as the threshold is relaxed. A low κ_{conn} means the gaps are already nearly equal — the sequence is "metrically uniform." A high κ_{conn} means large gap-ratio disparities must be accommodated before full connectivity is achieved.

Physical examples illustrate the contrast:

- **Simple polyatomics** (CH_4, CO_2, H_2O, NH_3, O_3): $\kappa_{\text{conn}} < 0.3$. The vibrational gap sequences of these symmetric molecules are metrically uniform — their gaps are nearly proportional and connect at near-zero threshold.
- **Cosmic web** (DESI rotated, $n = 1999$): $\kappa_{\text{conn}} = 15{,}658$. The void-dominated large-scale structure produces highly irregular gap sequences that require a large threshold to become connected.
- **He (QM-I)**: $\kappa_{\text{conn}} \approx 10^6$. The hydrogen-like spectral series of helium has a rapidly increasing gap sequence; the vulnerability graph connects only under extreme adaptive extension.

11.3 Constancy Across the Grid

Crucially, κ_{conn} is itself constant across the (α, μ) grid for every fixed dataset (a consequence of structural rigidity). The sub-regime metric structure is thus a property of the *ladder encoding*, not of the deformation parameters. This reinforces the general principle that representation determines structure.

12 Extended Corpus: Batches 2 and 3

12.1 New Domains

The Batch 3 corpus introduced five domains not previously represented in STRUC-PERC-I evaluations:

1. **Atmospheric dynamics (ERA5).** The ERA5 ECMWF reanalysis provides global gridded wind-field data. Eight ladder constructions (latitude-band maxima, signed means, global longitude sectors, top-12 jet stream levels) all return FULL with $\kappa_{\text{conn}} \leq 2.0$. The consistently low connectivity threshold indicates tight gap clustering in atmospheric wind profiles.
2. **Geoid harmonics (Earth, Mars, Moon).** Spherical harmonic gravity coefficients (EIGEN-6C4, JGM85, AIUB-GRL350A) evaluated at the physical $\alpha = 1.0$ point with μ-sweep: all FULL. The Realizability Anchoring Conjecture (that physical-α ladders preferentially realise FULL) is supported by this domain.
3. **Cosmic web (DESI, SDSS, 2MRS).** Angular orientation statistics of large-scale structure; μ-sweep at physical α. All 7 constructions FULL; connectivity delays (κ_{conn} up to 15,658) are the largest in the corpus and reflect the sparse, void-dominated nature of cosmic web density fields.

4. **Solar electromagnetic domain (GOES-XRS).** The first solar-domain evaluation. GOES X-ray solar flux energy levels produce a 7-gap ladder that returns FULL with $\kappa_{\text{conn}} = 16.6$ across the full 17×17 grid.

5. **Crystallographic structures (Materials Project).** Crystal lattice ladders from the Materials Project database. Verdict varies by normalisation convention (`cell_volume` vs. `per_atom`), providing a clean controlled representation split within a single physical domain.

12.2 Universality of the Core Results

All three corpus-level findings hold without exception across the extended corpus: zero verdict transitions, zero non-trivial commutators, 93/93 structurally rigid datasets. The representation dependence finding gains further evidence from the crystallographic normalisation split and the Zeeman-vs-QM-I updates in the revised atomic datasets.

13 Cross-Layer Interpretation

The phase-mapping results must be interpreted within the full two-coordinate structure of the UNNS framework. This section states the cross-layer conclusions and explicitly bounds their scope.

Corollary 6 (Local Operator Irrelevance — Corollary 4 instantiated)**.** *Within the tested domain $\Omega = [0.80, 1.20]^2 \subseteq \Omega_L$ for all corpus ladders:*

1. *The operators α and μ do not alter the realizability class of any tested ladder.*
2. *The operator order ($\alpha \circ \mu$ vs. $\mu \circ \alpha$) is structurally irrelevant for any tested ladder within Ω.*

This is the corpus instantiation of Corollary 4 of Principle 1.

Remark 10 (Compatibility with the Structural Response manuscript)**.** Theorem 6 does *not* contradict operator-sensitive behaviour documented in the Structural Response manuscript. The compatibility follows from the explicit domain restriction: the Structural Response work studies deformations of fundamental constants (α, μ_p, α_s, α_G) across physically meaningful ranges and reports domain-specific, non-trivial structural responses. The present phase-mapping protocol operates on ladder-level scale and shift parameters within $\pm 20\%$. These are different deformation spaces probing different aspects of structural sensitivity. The relationship is:

Layer	Deformation	Structural response
Phase Mapping	$(\alpha, \mu) \in [0.80, 1.20]^2$ (ladder-level)	Rigid over Ω
Structural Response	Fundamental constant variation	Sensitive; domain-specific

Rigidity within Ω is a bounded empirical fact about one deformation direction. It does not imply global structural insensitivity.

Remark 11 (Admissibility is not assessed here)**.** Phase-mapping rigidity is a statement about the *realizability coordinate* $\mathcal{R}(L)$ only. The present protocol does not evaluate the admissibility coordinate $\bar{\rho}(L)$ under (α, μ) deformation. Whether admissibility exhibits analogous rigidity under ladder-level scaling and shifting is an independent open question requiring a joint STRUC-I / STRUC-PERC-I deformation protocol.

14 Discussion

14.1 Relation to Percolation Theory

The vulnerability graph framework underlying STRUC-PERC-I is formally analogous to site or bond percolation on a complete graph, with a distance-based connection criterion parameterised by κ. The standard percolation picture predicts a sharp transition in giant component size at a critical threshold κ_c. The present results are not in contradiction with this: every FULL ladder exhibits such a transition (at its specific κ_{conn}). The new result is that κ_{conn} is itself invariant under (α, μ) deformation. The Connectivity-Margin Mechanism (Mechanism 1) explains this invariance as a consequence of the ladder's gap vector lying at a positive distance from any realizability boundary.

14.2 Relation to Renormalisation Group Ideas

Bounded Structural Rigidity bears a formal resemblance to renormalisation group fixed-point behaviour: the realizability class is stable under rescaling (the α operator) within the tested range. The Connectivity-Margin Mechanism provides a concrete, non-RG account of this stability: the decisive inequalities do not cross thresholds because the ladder has finite margin $m(L) > 0$. The analogy must not be over-extended. Standard RG analysis involves iterative coarse-graining transformations with non-trivial flow equations; here, α is a simple multiplicative rescaling of all ladder values, and its structural irrelevance within Ω is an empirical fact about the gap distributions of physical systems — not a consequence of scale-invariance of the edge criterion $|\Delta_i - \Delta_j| \leq \varepsilon(\kappa)$, which is not ratio-based. The rigidity is bounded: it does not extend to all scales.

14.3 Relation to the Dual Observability Framework

The phase-mapping results provide a clean separation between the two structural coordinates: admissibility (STRUC-I) and percolative realizability (STRUC-PERC-I). Structural rigidity under (α, μ) deformation is a STRUC-PERC-I property and does not directly imply anything about STRUC-I admissibility under the same deformation. A joint deformation protocol involving both instruments would be needed to assess whether admissibility exhibits analogous rigidity. The Connectivity-Margin Mechanism is specific to the realizability coordinate; it does not make predictions about the admissibility coordinate.

14.4 Limits of the Present Corpus

Several important limitations apply:

1. **Parameter range.** The tested range $[0.80, 1.20]$ spans $\pm 20\%$ around the physical value. Rigidity does not hold at all scales; the breakdown scans demonstrate fragmentation at amplified α.

2. **Operator family.** Only proportional scaling (α) and baseline shift (μ) are tested. Non-affine deformations, selective deletions, or parity projections produce qualitatively different behaviour and are not covered.

3. **Engine errors.** Three Al_2O_3 datasets produced no result; it is unknown whether they would satisfy rigidity.

4. **Corpus scope.** 93 datasets represent a substantial but not exhaustive survey of physical systems. Domains not yet tested include nuclear resonances at full density, biological genomic sequences, and seismic tomography ladders.

14.5 Open Questions

1. **Canonical ladder problem.** Is there a natural, physically motivated canonical encoding for each class of system that makes the structural verdict an invariant of the physical system? (Proposition 7.3 / open problem.)

2. **Phase transitions beyond** $[0.80, 1.20]$**.** Do any physical-system ladders exhibit a verdict transition for moderate deformations outside this range but within the physically accessible parameter space?

3. **Non-commutative systems.** Is there any ordered physical sequence for which $C(\alpha, \mu; L) \neq 0$? Constructing or discovering such a system would require a ladder near a structural boundary whose gap distribution responds asymmetrically to scale vs. shift deformations.

4. **Rigidity in higher-dimensional deformation space.** Does rigidity extend to joint deformations involving the strong coupling α_s or gravitational constant α_G?

5. **Universality of local rigidity.** Does every admissible ladder $L \in \mathcal{M}_{\text{adm}}$ possess a non-zero stability region $\Omega_L \neq \{(1, 1)\}$? (Conjecture 1.) A proof would elevate Principle 1 to a theorem. A counterexample — an admissible ladder with no neighbourhood of the physical point in which realizability is stable — would fundamentally revise our understanding of structural sensitivity.

6. **Sub-regime metric prediction.** Can κ_{conn} be predicted from structural properties of the gap sequence without running the full vulnerability-graph sweep?

15 Structural Interpretation of Realizability

The results of Sections 7–13 establish that the realizability coordinate $\mathcal{R}(L)$ is invariant under bounded deformation within the tested domain $\Omega \subseteq \Omega_L$. This invariance is not merely a numerical regularity, but reflects a deeper structural property of the observable itself.

The realizability coordinate does not behave as a continuous functional of the ladder under deformation. Instead, it exhibits *piecewise-invariant behaviour*: the deformation space is partitioned into regions within which $\mathcal{R}(L)$ remains constant, separated by boundaries across which discrete changes of class occur.

Accordingly, $\mathcal{R}(L)$ should not be interpreted as a smooth response variable, but as a *categorical structural observable* defined on stratified regions of deformation space. Within each such region, variations in the ladder induced by admissible deformation do not alter the connectivity relations that determine class membership.

This interpretation clarifies the empirical findings:

- The monochromatic phase maps observed in Section 6 correspond to a single such invariant region.
- The vanishing commutator (Section 8) follows from the constancy of the observable within that region.
- The sensitivity of realizability to representation (Section 9) reflects the fact that different encodings may lie in different regions of this partition.

Thus, the central outcome is not simply invariance under deformation, but the identification of realizability as a piecewise-invariant structural observable defined by region-wise stability.

16 Boundary Behaviour and Regime Transition

The existence of a local stability region Ω_L (Principle 1) implies the presence of a boundary $\partial\Omega_L$ in deformation space at which realizability transitions may occur.

Within Ω_L, the decisive connectivity relations underlying class membership are preserved, and the realizability coordinate remains invariant. At the boundary $\partial\Omega_L$, these relations reach critical configurations at which the connectivity structure changes in a manner sufficient to alter the realizability class.

Transitions are therefore not gradual. A change in realizability class requires a *boundary-crossing event*, in which the ladder crosses a threshold separating distinct connectivity regimes. Such events correspond to the appearance or disappearance of decisive structural features, such as:

- the formation or loss of a dominant backbone,
- the isolation or integration of outlier gaps,
- or the reconfiguration of component structure at critical scales.

Beyond the boundary, in $\mathbb{R}^2 \backslash \Omega_L$, the ladder may enter a different realizability regime, as observed in extended deformation studies (e.g., geoid harmonics at amplified α; Section 12).

This boundary-based interpretation reconciles the present results with those of the Structural Response manuscript: local rigidity within Ω_L is compatible with sensitivity under larger or qualitatively different deformations that move the system across $\partial\Omega_L$.

17 Geometry of Deformation Space

The phase-mapping results imply a specific geometric structure of deformation space.

The (α, μ)-plane does not support a smooth response manifold for realizability. Instead, it is naturally partitioned into a collection of regions within which $\mathcal{R}(L)$ is constant, separated by boundaries at which discrete transitions occur. The resulting structure is therefore *stratified*, rather than continuous.

Each ladder L induces a partition of deformation space into:

- **rigidity domains**, within which $\mathcal{R}(L)$ is invariant;
- **transition loci**, forming the boundaries between such domains.

Within rigidity domains, variations of (α, μ) do not alter the connectivity structure. At transition loci, the system becomes sensitive to deformation, and small changes may produce discontinuous changes in realizability.

The observed phase maps correspond to a single rigidity domain intersecting the tested region Ω. The absence of transitions and commutator effects within this region reflects the fact that Ω lies entirely within one stratum of the partition.

This geometric interpretation provides a natural language for describing both the present results and their extension: the study of realizability under deformation becomes the study of the stratification of deformation space induced by connectivity structure.

18 Relation to Stability in Physical and Mathematical Systems

The bounded structural rigidity identified here differs in important ways from classical notions of stability.

In many physical and mathematical systems, stability is understood as the continuous persistence of properties under small perturbations, often accompanied by smooth variation of observables. In contrast, the present results indicate that realizability is governed by *thresholded structural conditions*.

The invariance observed within Ω_L does not arise from smooth dependence, but from the fact that the system remains within a region of deformation space in which the decisive inequalities defining connectivity are preserved. When these inequalities are violated, the system does not undergo gradual change, but rather transitions discretely to a different regime.

In this sense, realizability exhibits a form of *structural stability without continuity*: it is stable within regions, but changes discontinuously across their boundaries.

This behaviour is reminiscent of stratified or piecewise-defined systems, but is here derived from the specific structure of gap-based connectivity and the percolative realizability framework. The resulting notion of stability is therefore distinct from both classical perturbative stability and purely topological invariance, and is instead grounded in the thresholded organisation of gap space.

19 Program for Empirical Expansion

The identification of bounded structural rigidity and the connectivity-margin mechanism (Mechanism 1) suggests a concrete program for further investigation.

19.1 Quantitative Characterisation of the Margin

A central objective is the quantitative characterization of the proposed margin functional $m(L)$, measuring the distance of a ladder from realizability class boundaries. This requires:

1. operational definition of $m(L)$ within the STRUC-PERC-I framework,
2. computation of $m(L)$ across the existing corpus,
3. and analysis of its relation to observed rigidity and breakdown behaviour.

19.2 Search for Near-Boundary Ladders

A second direction is the systematic search for near-boundary ladders, for which $m(L)$ is small. Such systems are expected to be the most sensitive to deformation and therefore the most likely to exhibit:

- non-monochromatic phase maps,
- non-zero commutators,
- or early breakdown under extended deformation.

19.3 Further Extensions

Additional directions include:

- exploration of additional operator classes beyond uniform affine deformation,
- refinement of realizability boundary conditions in terms of gap structure,
- and integration of these results with the broader operator framework of the UNNS Substrate (see Structural Response manuscript).

These directions form a natural continuation of the present work, aimed at transforming the current principle-level results into quantitative and, ultimately, theorem-level statements.

20 Strategy for Falsification

The principle of bounded structural rigidity (Principle 1) and the associated mechanism candidate (Mechanism 1) are empirically supported by the present corpus, but remain subject to falsification.

20.1 Falsification of the Principle

A direct falsification of Principle 1 would require the identification of a ladder L for which arbitrarily small admissible deformation produces a change in realizability class. Such a ladder would have no non-zero stability region Ω_L, contradicting the principle.

20.2 Falsification of the Margin Functional

For the connectivity-margin mechanism, falsification proceeds differently. The proposed margin functional $m(L)$ is intended to capture the distance to realizability boundaries. If a ladder is found for which the operational definition yields $m(L) = 0$, yet a non-zero rigidity region is observed, then the functional is insufficient and must be refined.

20.3 Practical Strategies

Practical strategies for falsification therefore focus on:

- constructing or identifying ladders with highly irregular or multi-scale gap structures,
- examining systems with closely spaced gap clusters,
- and performing fine-grained deformation studies in regions suspected to be near $\partial\Omega_L$.

Such investigations are essential for determining whether the observed rigidity is a universal structural property or a widespread but ultimately contingent feature of the current corpus.

21 Conclusion

We have presented the first large-scale systematic phase-mapping study of structural regimes in the UNNS Substrate framework. Using a fully automated evaluation pipeline (field generator) coupling a Python orchestration layer to the STRUC-PERC-I engine via a Puppeteer-bridged Node.js RPC, we evaluated 93 ladder datasets across 11 physical domains at 22,817 (α, μ) grid points.

The corpus supports three central findings:

1. Bounded Structural Rigidity of Realizability (Principle 1). The corpus supports Principle 1: for every tested admissible ladder, the tested domain $\Omega = [0.80, 1.20]^2$ lies within the realizability stability region Ω_L. No inter-class transition is observed across 93 datasets and 22,817 evaluations. The principle is local (applies within Ω_L, not globally), ladder-dependent (Ω_L varies with L), and coordinate-restricted (concerns $\mathcal{R}(L)$ only). Whether every admissible ladder possesses a non-trivial Ω_L is Conjecture 1 — open.

2. Emergent Commutativity (Corollary 3). The structural commutator $C(\alpha, \mu; L) = \mathbf{0}$ at every evaluated grid point — a direct corollary of Principle 1, not an independent result. Operator order is irrelevant within Ω_L and may be non-trivial outside it, consistent with the Structural Response manuscript.

3. Representation as the Primary Structural Variable. While deformation within Ω does not alter the realizability class of a fixed ladder, the choice of encoding does — sometimes categorically. Cross-representation splits (He, Na, HD, geoid, crystallographic) demonstrate that realizability class is a joint property of physical system and encoding (Theorem 2). The canonical ladder problem remains open.

Final Position. Structural rigidity observed in phase mapping is a *bounded local property of the realizability coordinate under joint* (α, μ) *deformation within* Ω_L, not a universal invariance of structural systems. The full two-coordinate description $\mathcal{S}(L) = (\bar{\rho}(L), \mathcal{R}(L))$ remains necessary; the present results characterise one coordinate ($\mathcal{R}$) under one class of deformation, inside the larger layered hierarchy: USL $\rightarrow$ admissibility $\rightarrow$ realizability $\rightarrow$ dynamics.

Closing statement. The central outcome of this work is the identification of realizability as a locally rigid structural observable, governed not by continuous response but by discrete boundary conditions in gap space.

Data and Code Availability. All corpus evaluations are produced by the field generator pipeline (Python + Node.js + STRUC-PERC-I v2.4.0/2.4.1). Engine source at `struc_perc_i_v2_4_0.html` (UNNS project repository). Full corpus results in JSON format available on request.

A Protocol Theorem Reference and Manuscript Cross-Index

The table below maps each theorem of the Phase Mapping Protocol to its empirical status in the present corpus, the corresponding manuscript theorem, and the relevant section. All Protocol theorems use realizability-class language consistent with the PRP framework.

Protocol	Name	Statement	Corpus Status	Manuscript ref.
T1	Regime Stability	$\mathcal{C}(L)$ invariant over $\Omega \Rightarrow$ L structurally stable.	Satisfied: 93/93	Thm. 3
T2	Structural Commutativity	$C(\alpha, \mu; L) = \mathbf{0}$ for all $(\alpha, \mu) \in \Omega$.	Satisfied: 93/93	Thm. 5
T3	Hidden Variation	$\Delta_{\mathcal{C}} = 0$ but $\Delta_{\kappa} \neq 0 \Rightarrow$ sub-regime variation.	Observed between datasets	Thm. 4
T4	Phase Transition	$\mathcal{C}$ changes discontinuously near (α^*, μ^*).	Not observed in Ω	Rem. 5
T5	Structural Rigidity	$\mathcal{C}$ constant and $C = \mathbf{0}$ over Ω.	Satisfied: 93/93	Thm. 1
T6	Operator Sensitivity	$\exists\, (\alpha, \mu) \in \Omega$ such that $C \neq \mathbf{0}$.	Not observed in Ω	Rem. 6
T7	Regime Boundary	$\partial\Omega_{\mathcal{C}} = \{(\alpha, \mu) :$ $\mathcal{C}$ changes$\}$.	Empty within Ω	Sec. 6
T8	Phase Map	$\Phi : (\alpha, \mu) \mapsto \mathcal{C}$ defines the structural phase diagram.	Degenerate (constant) for all 93	Sec. 6
C1	Degenerate Phase Space	$\Phi = \mathcal{C}_0$ constant $\Rightarrow$ Ω phase-degenerate.	Satisfied: 93/93	Thm. 1
C2	Non-Commutative Region	Region where $C \neq \mathbf{0}$ exists.	Empty within Ω; open beyond	Sec. 14.5
New manuscript results (Principle 1 and its corollaries)				
—	Principle 1 (BSR of $\mathcal{R}$)	$\exists\, \Omega_L \ni (1,1)$: $\mathcal{C}$ and G_{κ} invariant over Ω_L.	Corpus-supported (93/93)	Prin. 1
—	Corollary 1 (Deg. Phase Space)	$\Phi_L = \mathcal{C}(L)$ within Ω_L.	Satisfied: 93/93	Cor. 2
—	Corollary 2 (Emergent Commutativity)	$C(\alpha, \mu; L) = \mathbf{0}$ within Ω_L.	Satisfied: 93/93	Cor. 3
—	Corollary 3 (Operator Irrelevance)	Order and magnitude irrelevant within Ω_L.	Satisfied: 93/93	Cor. 4
—	Conjecture (Universality)	Every $L \in \mathcal{M}_{\text{adm}}$ has $\Omega_L \neq \{(1,1)\}$.	Open	Conj. 1
—	Repr. Dependence of $\mathcal{R}$	$\mathcal{C}(L_1) \neq \mathcal{C}(L_2)$ for same system, diff. encoding.	Documented: He, Na, HD, crystals	Thm. 2

B Field Generator: Source Code Summary

The field generator pipeline consists of the following modules:

File	Role
`config.py`	Grid definitions (α, μ ranges), operating mode switch (`UNNS_MODE`), engine path, dataset auto-discovery.
`analysis.py`	Normalisation of engine output schema (snake_case $\leftrightarrow$ camelCase), commutator computation (Δ_{GR}, Δ_κ, Δ_V), transition detection.
`engine_bridge.py`	Long-lived `StrucPercEngine` process object; stdin/stdout JSON RPC to Node.js server; blocking `run(ladder)` call.
`engine_server.js`	Puppeteer headless Chromium; loads STRUCPERC-I HTML as local file; exposes `window.runAnalysisFromData(ladder)` via page evaluation; line-oriented JSON protocol.
`convert_csv_to_txt.py`	Utility: converts CSV ladder files to whitespace-separated TXT.
`config_breakdown.py`	Alternate configuration for the breakdown scan mode ($\alpha \in [1.0, 4.0]$).

Operating mode is controlled by the environment variable `UNNS_MODE`:

- `python runner.py` — phase-mapping mode (17×17 grid).
- `UNNS_MODE=break python runner.py` — breakdown scan.
- `UNNS_MODE=mu python runner.py` — μ-sweep at physical α.
- PowerShell: `$env:UNNS_MODE="break"; python runner.py`

C Corpus Dataset Index

Table 1: Full corpus dataset index (93 datasets).

Dataset	Domain	Verdict	κ_{conn}
Batch 1 — Atomic / Molecular / Nuclear (34 datasets)			
He (QM-I)	Atomic	FULL	$\approx 10^6$
Li (QM-I)	Atomic	FULL	376,546
Na (QM-I)	Atomic	HARD	—
K (QM-I)	Atomic	FULL	—
He (Zeeman)	Atomic	TAIL	—
Na (Zeeman)	Atomic	HARD	—
H (Zeeman, $n = 1999$)	Atomic	HARD	—
Li (Zeeman)	Atomic	FULL	—

Dataset	Domain	Verdict	κ_{conn}
K (Zeeman)	Atomic	FULL	—
CO (combined)	Molecular	HARD	—
CO_2	Molecular	FULL	< 0.3
CH_4	Molecular	FULL	< 0.3
H_2O	Molecular	FULL	< 0.3
NH_3	Molecular	FULL	< 0.3
O_3	Molecular	FULL	< 0.3
HD (combined)	Molecular	HARD	—
HD (lower)	Molecular	FULL	—
HD (upper)	Molecular	FULL	—
HD (even)	Molecular	FULL	—
HD (odd)	Molecular	HARD	—
(U-238 and remaining B1 datasets — details in primary output JSON)			
Batch 2 — CMB (3 datasets)			
CMB TT (Planck R3.01, $n = 399$)	CMB	FULL	7.9
CMB TE (Planck R3.01, $n = 499$)	CMB	FULL	1.0
CMB EE (Planck R3.01, $n = 54$)	CMB	FULL	1.0
Batch 3 — Atmosphere / Geoid / Cosmic Web / Solar / Crystallography (56 datasets)			
ERA5 latband absmax	Atmosphere	FULL	0.7
ERA5 latband signedmean	Atmosphere	FULL	1.0
ERA5 global lonsector	Atmosphere	FULL	2.0
ERA5 top-12 jet stream	Atmosphere	FULL	2.0
(4 additional ERA5 constructions — all FULL*)*			
EIGEN-6C4 Earth ($n = 181$)	Geoid	FULL	1.0
JGM85 Mars ($n = 499$)	Geoid	FULL	0.7
AIUB-GRL350A Moon ($n = 142$)	Geoid	FULL	6.3
DESI full synthetic ($n = 666$)	Cosmic web	FULL	5,908
DESI rotated ($n = 1999$)	Cosmic web	FULL	15,658
SDSS (n varies)	Cosmic web	FULL	27.9
2MRS (6 constructions)	Cosmic web	FULL	varies
GOES-XRS solar	Solar	FULL	16.6
(Materials Project crystallographic datasets — 15 valid, 3 excluded)			